

Monthly quasi-periodic eruptions from repeated stellar disruption by a massive black hole

P.A. Evans¹ C.J. Nixon^{2,1} S. Campana³ P. Charalampopoulos^{4,5} D. A. Perley⁶ A.A. Breeveld⁷ K.L. Page¹ S.R. Oates⁸ R.A.J. Eyles-Ferris¹ D.B. Malesani^{9,10,11} L. Izzo^{11,12} M.R. Goad¹ P.T. O'Brien¹ J.P. Osborne¹ B. Sbarufatti³

In recent years, searches of archival X-ray data have revealed galaxies exhibiting nuclear quasi-periodic eruptions with periods of several hours. These are reminiscent of the tidal disruption of a star by a supermassive black hole, and the repeated, partial stripping of a white dwarf in an eccentric orbit around a $\sim 10^5 M_\odot$ black hole provides an attractive model. A separate class of periodic nuclear transients, with significantly longer timescales, have recently been discovered optically, and may arise from the partial stripping of a main-sequence star by a $\sim 10^7 M_\odot$ black hole. No clear connection between these classes has been made. We present the discovery of an X-ray nuclear transient which shows quasi-periodic outbursts with a period of weeks. We discuss possible origins for the emission, and propose that this system bridges the two existing classes outlined above. This discovery was made possible by the rapid identification, dissemination and follow up of an X-ray transient found by the new live *Swift*-XRT transient detector, demonstrating the importance of low-latency, sensitive searches for X-ray transients.

1 Introduction

Swift J023017.0+283603 (hereafter *Swift* J0230) was discovered in *Swift*-X-ray Telescope (XRT) data by the Living *Swift*-XRT Point Source (LSXPS) catalogue's real-time transient detector¹ on 2022 June 22². The source was serendipitously present in an observation of an unconnected source, SN 2021afk (4.3' away), and had a 0.3–10 keV count rate of $2.7_{-0.5}^{+0.6} \times 10^{-2}$ ct s⁻¹. This field had been observed on 11 previous occasions by *Swift* between December 2021 and January 2022; combining all of those observations, *Swift* J0230 was undetected down to a 3- σ upper limit of 1.5×10^{-3} ct s⁻¹. The last of these observations was 164 days before the discovery of *Swift* J0230, placing a rather loose lower limit on its switch-on time; for convenience we give all times relative to MJD 59752 (midnight on the day of discovery). The best localization of *Swift* J0230 is from the XRT, and is RA=02^h 30^m 17.12^s, Dec=+28° 36' 04.4" (J2000), with an uncertainty of 2.8" (radius, 90% confidence). This is consistent with the nucleus of the galaxy 2MASX J02301709+2836050, but also marginally consistent with the type-II supernova SN2020rht (3.1" away), discov-

ered two years earlier on 2020 August 12³ (Figure 1). An optical spectrum of 2MASX J02301709+2836050, obtained with the Nordic Optical Telescope (Figure 2), gives a redshift $z = 0.03657 \pm 0.00002$. Assuming standard cosmological parameters⁴, this corresponds to a luminosity distance $D_L = 160.7$ Mpc. The galaxy type is unclear, but it is either quiescent or, at most, a very weak AGN (see the Supplementary Information).

2 Results

2.1 X-ray analysis Following the initial, serendipitous discovery, we obtained regular monitoring with *Swift* (see the Methods section for details). The initial outburst continued for 4 days following the discovery; on the fourth day it ended with a rapid decay, the luminosity falling by a factor of 20 in just 57 ks; there was a brief rebrightening (a factor of 4.5 in 6 ks), before it became too faint to detect; the light curve is shown in Figure 3. Fitting this decay with a power-law, $L \propto (t - t_0)^{-\alpha}$ (where t_0 is set to the start of the first bin in this observation), gives $\alpha = 11.0 \pm 1.7$. Eight subsequent outbursts were observed at ~ 25 d intervals, with durations ~ 10 –15 d. The fifth outburst was either significantly longer (up to ~ 32 d), or consisted of a weak outburst, a return to quiescence, and then a second, longer outburst. This was followed by a long gap of ~ 70 d during which two possible short and weak outbursts were seen, before another outburst similar to the early ones.

A Lomb-Scargle analysis (see Methods and Extended Data Figure. 1) reveals moderately-significant peaks at approximately 22 and 25 d periods, although each peak is ~ 1 d wide, confirming the quasi-rather than strictly-periodic nature of the variability, as may be expected from eyeballing the light curve. Further consideration of the variability requires us to define what constitutes an outburst: the initial outburst and that from days ~ 41 –48 appear clearly defined, but during the outburst from days ~ 60 –75, the source underwent a sudden decline, being undetected on day 72 with an upper limit of $L < 8.9 \times 10^{41}$ erg s⁻¹ (0.3–2 keV), recovering to $L \sim 2 \times 10^{42}$ erg s⁻¹ by day 74. It seems plausible to interpret this as a single outburst, with a sudden, brief dip. Hereafter, what constitutes an outburst becomes more subjective. The outbursts starting on days 89 and 102 could each be explained as comprising two short outbursts close together, or a single outburst with a quiet phase in the middle; it is worth noting that in the first of these, if we sum the upper limits during this quiet phase, we find a detection at a higher level than the upper limits found in the quiescent phases. During the long, largely quiescent period from days 111–195 the source was twice briefly detected with $L \sim 1 - 2 \times 10^{41}$ erg s⁻¹, but these are hardly 'outbursts' in the same way as the earlier emission. Based on visual inspection of the light curve, we define an outburst as comprising any times where $L > 2 \times 10^{41}$ erg s⁻¹; the details of the outbursts thus identified are given in Table 1 – see the Methods section for full details of how these were derived. In summary: we have de-

¹School of Physics and Astronomy, University of Leicester, University Road, Leicester, LE1 7RH, UK; pae9@leicester.ac.uk ²School of Physics and Astronomy, University of Leeds, Woodhouse Ln, Leeds, LS2 9JT, UK ³INAF, Osservatorio Astronomico di Brera, via E. Bianchi 46, 23807, Merate, Italy ⁴Department of Physics and Astronomy, Tuorla Observatory, University of Turku, FI-20014, Turku Finland ⁵DTU Space, Technical University of Denmark, Elektrovej 327, 2800, Kongens Lyngby, Denmark ⁶Astrophysics Research Institute, Liverpool John Moores University, IC2, Liverpool Science Park, 146 Brownlow Hill, L3 5RF, Liverpool, UK ⁷Mullard Space Science Laboratory, University College London, Holmbury St Mary, RH5 6NT, Dorking, UK ⁸School of Physics and Astronomy & Institute for Gravitational Wave Astronomy, University of Birmingham, B15 2TT, Birmingham, UK ⁹Department of Astrophysics/IMAPP, Radboud University, 6525 AJ Nijmegen, The Netherlands ¹⁰Cosmic Dawn Center (DAWN), Denmark ¹¹Niels Bohr Institute, University of Copenhagen, Jagtvej 128, 2200, Copenhagen N, Denmark ¹²INAF-Osservatorio Astronomico di Capodimonte, Salita Moiariello 16, 80131, Napoli, Italy

ected transient X-ray emission that rapidly switches on and off again with a recurrence timescale that is of the order of 25 d, but which can vary by several days between outbursts. The duration of the outbursts also shows significant variability with the longest being of order 20 days and the shortest less than a day.

The X-ray spectrum during the outbursts was very soft, with no emission seen above 2 keV, and could be well-modelled with a simple blackbody emitter with only Galactic absorption. Due to this soft spectrum, the typical energy bands used for XRT hardness ratios were inappropriate; we selected 0.3–0.9 keV and 0.9–2 keV as this gave roughly equal counts in the two bands, maximising the signal-to-noise ratio. The time-evolution of this hardness ratio (Figure 3) shows a clear correlation between luminosity and spectral hardness (Spearman rank p -value of 1.3×10^{-6} of the data being uncorrelated), ruling out a change in absorption as the cause of the flux variation. We fitted the absorbed blackbody model to each observation in which Swift J0230 was detected. The blackbody temperature obtained is strongly correlated with luminosity (p -value: 4.5×10^{-6} ; see Extended Data Figure. 2); no evidence for absorption beyond the Galactic column is seen.

As noted earlier, while coincident with the galaxy nucleus, the XRT position is also potentially in agreement with that of SN 2020rht. We obtained a 3 ks *Chandra* DDT observation during the fourth outburst to obtain a better position, but unfortunately this observation fell on day 97, which turned out to be in one of the mid-outburst quiet phases.

2.2 Optical and UV analysis At optical and ultraviolet wavelengths, there is no evidence for outbursting behaviour. We obtained data from both *Swift* UV/Optical Telescope (UVOT) and the Liverpool Telescope (Extended Data Tables 1–2). The host galaxy, 2MASX J02301709+2836050, is clearly detected in all observations, but there is no evidence for variability or an increase in flux compared to catalogued values. For UVOT, we also analysed the data from the pre-discovery observations and find no secure evidence for a change in brightness between those data and the observations taken during outburst. Full details are given in the Methods section.

3 Discussion

The peak luminosity of $\sim 4 \times 10^{42}$ erg s $^{-1}$, the timescales of the outbursts and their quasi-periodic, quasi-chaotic nature, the soft X-ray spectrum and lack of optical variability place significant constraints on the possible models to explain Swift J0230. While the lack of detection with *Chandra* means that we cannot rule out a positional association with SN2020rht, it is difficult to see how a supernova could have evolved into the object which we have detected. The spectrum, luminosity and variability timescale are inconsistent with the properties of ultra-luminous X-ray sources⁵, and while certain supernovae could in principle be followed by X-rays from a newly-formed millisecond pulsar⁶, this should occur while the supernova is still visible in the optical.⁷ have shown how this emission could be delayed, but the timescales and luminosities they predict (e.g. their fig. 5) are not consistent with our observation. Equally, neither model explains the variability or spectrum we see in Swift J0230. We discuss this further in the Supplementary Information.

We suggest that (near) periodic mass supply into an accretion flow onto the central supermassive black hole in 2MASX J02301709+2836050 presents the most likely explanation for Swift J0230. From simple energetics (see Supplementary Information) we can infer that the total mass accreted during a typical outburst is $\sim 10^{-5} M_{\odot}$. In an AGN, a supermassive black hole at the heart of a galaxy accreting from a surrounding disc of gas, flares and outbursts are common. However, the timescale and spectrum of Swift J0230 are not consistent with typical AGN behaviour, and 2MASX J02301709+2836050 itself does not appear to be an AGN (Extended Data Figure. 3; see Supplementary Information for a full discussion).

We therefore consider the possibility that one (or several) stars are interacting with, and feeding mass on to, the central supermassive black hole. One possible mechanism for producing the mass flow is the interaction of two stars in orbit around the black hole; if they pass sufficiently close to each other material can be liberated from one or both stars that can feed the central black hole^{8,9}. To generate the required timescales from this model requires a pair of stars orbiting in the same direction and in the same plane⁹. This could occur for stellar orbits that are initially randomly oriented if they can be subsequently ground down into the same plane by interaction with an AGN disc¹⁰. For Swift J0230, which lacks any clear signature of a standard AGN disc, it is unlikely that any stars orbiting the central black hole have the required orbits to achieve the observed timescales.

Another possibility is a repeating, partial Tidal Disruption Event (rpTDE), in which a star on a bound, highly-eccentric orbit loses some of its envelope every pericentre passage due to tides from the black hole’s gravitational field. These events are a sub-class of TDEs in which the “regular” scenario sees the incoming star approach the black hole on a parabolic orbit, and the star is destroyed by the first encounter (see refs^{11,12} for reviews of TDEs).

The rpTDE model was investigated prior to the discovery of any corresponding sources (for example, ref¹³) and was suggested as the explanation of X-ray flares in the active galaxy IC 3599¹⁴. Recently, it has been proposed (for example, refs^{15–17}) as a possible explanation for hours-long quasi-periodic eruptions (QPEs) discovered in galactic nuclei (for example, refs^{18–22}). These works focused on the possibility of a white dwarf interacting with a relatively low-mass central black hole of mass $\sim 10^{5-6} M_{\odot}$. A second set of sources show much longer outbursts (both in duration and recurrence period) and have been referred to as periodic nuclear transients (PNTs); these may be the same rpTDE mechanism acting with a main-sequence star rather than a compact star^{23–26}, and a more massive black hole ($\sim 10^{7-8} M_{\odot}$).

In the rpTDE model, the donor star is in a highly eccentric orbit around a black hole; at each pericentre passage the star has to approach, but not quite reach, the tidal radius at which the star would be fully disrupted. The outer layers of the star are liberated, and some of this material accretes on to the central black hole powering the outburst. The recurrence time of the outbursts is related to the orbital period of the star. The majority of the energy released from the accretion process occurs in the central regions near the black hole where the matter is most likely in the form of an accretion disc. We can therefore provide an estimate of the black hole mass in Swift J0230 by comparing the temperature of ~ 100 eV ($\sim 10^6$ K), measured from the X-ray spectrum, with the peak temperature of a standard accretion disc²⁷. This yields (see the Supplementary Information) a black hole mass estimate of $\sim 2 \times 10^5 M_{\odot}$. This is similar to the mass estimates for the QPE sources (for example, refs^{18,19,22}). It is worth noting that the QPE sources and Swift J0230 show very little in the way of optical emission, whereas the PNTs show strong optical emission. This may simply reflect the difference in the black hole masses, i.e. the soft X-ray spectrum and the lack of optical emission seen in Swift J0230 appears consistent with this estimate of the black hole mass.

If the accreted material is stripped from the orbiting star during pericentre passage of a highly elliptical orbit, and the pericentre distance is a few gravitational radii (required to liberate any material from the surface of a white dwarf for black hole masses of a few $\times 10^5 M_{\odot}$), then we would expect the outburst duration to be similar in different systems, regardless of their orbital (and hence outburst) period. This is because the pericentre passage of a highly elliptical orbit is approximately that of a parabolic orbit and its duration is not connected to the orbital period. This means that it is difficult to explain both Swift J0230 (outburst duration of days) and the pre-existing QPEs (outburst duration of hours) as rpTDE of a white dwarf around a modest-mass

black hole. On the other hand, rpTDE of main-sequence stars by $\sim 10^7 - 10^8 M_\odot$ black holes have been proposed to explain the PNTs ASASSN-14ko, for which the recurrence timescale is 114 d^{23,24}, and AT2018fyk which exhibited a significant re-brightening after around 600 d of quiescence²⁵. Swift J0230 clearly lies between these two classes of object.

An important question is how the star arrived on such an orbit around the central black hole. Tidal capture, in which an orbiting star loses orbital energy due to tidal forces and becomes bound to the black hole²⁸, is typically incapable of generating the required orbits; however, the Hills mechanism²⁹ was proposed as a viable formation route for the PNT ASASSN-14ko³⁰. In this mechanism, a binary star system approaches the black hole with a small enough pericentre distance such that the tidal force from the black hole is stronger than the gravitational force holding the binary together. This results in the binary being disrupted, with one component ejected from the system, and the other locked into a bound, but highly eccentric, orbit about the black hole. If the progenitor of Swift J0230 were a binary consisting of a low mass, main-sequence star and, say, a white dwarf, then the main-sequence star needs to be captured into a bound orbit around the black hole with the observed ~ 25 d period. For a black hole mass of $M_\bullet \sim 4 \times 10^5 M_\odot$ this period corresponds to the most likely outcome of Hills capture from such a binary system (the calculations of³⁰ show that higher black hole masses are allowed but are significantly less likely to result in this period for the bound star; see Supplementary Information for details). This is consistent with the mass estimate derived from the temperature of the X-ray spectrum. Further, the expected accretion timescales from such a system (see Supplementary Information) are also consistent with those observed in Swift J0230.

The variable shape and timescales of the outbursts seen in Swift J0230 may also be explained by this model. In a standard TDE, as opposed to an rpTDE, the star arrives on a parabolic orbit, meaning that some of the stellar matter is bound to the black hole (the inner tidal stream), and this material forms an accretion flow, while the rest of the stellar debris (the outer tidal stream) is unbound and leaves the system¹¹. In an rpTDE, the star must be on a bound orbit around the black hole. In this case both the inner and outer tidal streams can remain bound to the black hole. The inner stream falls back soonest, and thus with a higher mass return rate, while the outer stream can return on longer timescales. Due to relativistic precession of the stellar debris orbits (both apsidal and nodal) the returning streams can collide and partially cancel their angular momenta to augment the accretion rate on to the black hole, with the magnitude of the effect depending on the orientation of the colliding orbits (see^{31,32} for similar variability induced in accretion discs due to relativistic precession; and the processes described therein may also occur in the discs formed in Swift J0230). The exact details of this interaction between the two streams, the accretion flow, and the orbiting star are complex and require a full numerical analysis which is beyond the scope of this discovery paper; however it is clear that such interaction will produce variable emission that could at least partially erase the more exactly periodic nature of the stellar orbit. An example of such complex interacting debris streams can be seen in fig. 9 of³³. It will be particularly important to determine if the star itself can be sufficiently perturbed during each pericentre passage, with e.g. tides imparting variations in oscillation amplitudes and rotation frequency, to change the amount of mass transferred and the structure of each outburst. Additionally, the sharp decline observed at the end of each outburst may be driven by the returning star disturbing the accretion flow. These questions can be addressed with future theoretical investigations.

We have proposed a single explanation for the QPEs and PNTs, as repeated, partial tidal disruption of a star in an eccentric orbit around a supermassive black hole; and reported the discovery of the first object

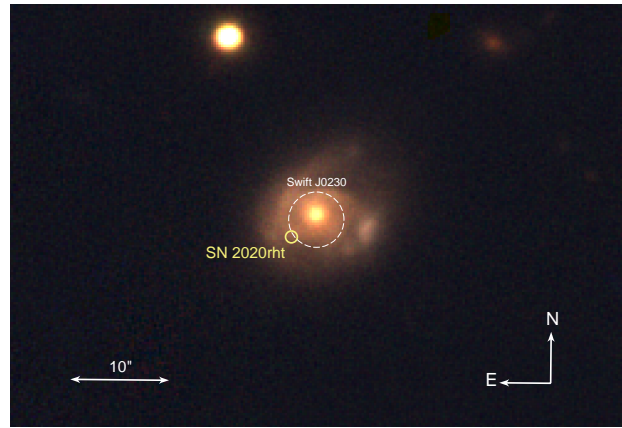


Figure 1 – The location of the new transient, Swift J0230, relative to its host galaxy and an old supernova. The image is an archival Pan-STARRS³⁶ image of 2MASX J02301709+2836050, with colour scaled arbitrarily for aesthetic purposes. The broken circle shows the 90% confidence *Swift*-XRT position of Swift J0230; the solid one SN 2020rht.

that can bridge the gap between these classes. The QPEs are thought to harbour a white dwarf and a modest ($\sim 10^5 M_\odot$) black hole, and the PNTs are thought to host a main sequence star and a more massive ($\sim 10^7 M_\odot$) black hole. Swift J0230 represents an intermediate class of system which is consistent with a main sequence star orbiting a modest-mass black hole. Given the timescales, modest fluxes, and lack of emission outside of the X-ray band, Swift J0230-like systems are difficult to discover. Unlike QPEs, which were discovered in archival data, their timescales and behaviour would not be exposed by a single observation. It is only with the recent creation of a real-time transient detector¹ that objects like this can be found rapidly enough for follow-up observations to expose their behaviour. The fact that this event was found within three months of enabling this real-time search suggests that they are reasonably common and we can expect to discover more objects of this class with sensitive, wide-field X-ray instruments such as *eRosita*³⁴ and in the near future, the *Einstein Probe*³⁵.

Methods

Discovery

At 13:58 UTC on 2022 June 22, the LSXPS real-time transient detector¹ reported the discovery of a possible new X-ray transient, dubbed Swift J023017.0+283603. The object was detected in *Swift* observation 00014936012 which had taken place between 08:19 and 08:46 UTC; i.e. the notification was produced 5.2 hours after the observation (most of this latency related to the timing of ground station passes and the ingesting of the data by the Swift Data Center: the observation data were received at the UKSSDC at 13:51 UTC). No catalogued X-ray source was found at this position. Further, *Swift* had already observed this location on 11 previous occasions (the observation target was SN2021afkk, 4.3' away from this serendipitous transient), for a total of 9.6 ks. These observations had been analysed as a stacked image in LSXPS (DatasetID: 19690); no source was present near the position of Swift J0230, with a 3- σ upper limit of 1.5×10^{-3} ct s⁻¹. The peak count rate of Swift J0230 in the new observation was $2.7^{+0.6}_{-0.5} \times 10^{-2}$ ct s⁻¹ (1- σ errors), significantly above this upper limit, clearly indicating that a new transient had been discovered.

Due to the very soft spectrum and coincidence with the nucleus of the galaxy 2MASX J02301709+2836050, this was originally interpreted as a tidal disruption event^{2,37}, and a high-urgency target-of-opportunity (ToO) request was submitted to *Swift*.

Table 1 – Constraints on the timescales of the observed outbursts. *The final outburst was ongoing when observations ended.

Outburst	Start		End		MJD		Duration		Period	
	MJD min	MJD max	MJD min	MJD max	min (d)	max (d)	min (d)	max (d)	min (d)	max (d)
1	59587.9	59752.3	59757.3	59757.4	4.9	169.5	10.9	185.1	10.9	185.1
2	59763.2	59773.0	59773.1	59787.5	0.1	24.3	0.1	24.3	10.9	185.1
3	59787.5	59793.7	59799.8	59800.4	6.2	12.9	6.2	12.9	14.5	30.4
4	59811.0	59815.3	59826.4	59827.0	11.1	16.0	11.1	16.0	17.3	27.8
5	59839.2	59841.5	59862.3	59867.5	20.8	28.3	20.8	28.3	24.0	30.5
6	59870.8	59886.7	59886.7	59887.9	0.0	17.0	0.0	17.0	29.3	47.5
7	59908.3	59909.7	59909.7	59910.8	0.0	2.4	0.0	2.4	21.6	38.9
8	59942.3	59948.0	59954.3	59955.6	6.4	13.4	6.4	13.4	32.5	39.6
9	59960.2	59963.0	59971.7	59974.8	8.7	14.7	8.7	14.7	12.2	20.7
10	60010.8	60011.9	60022.4*	—	11.6*	—	11.6*	—	47.8	51.8

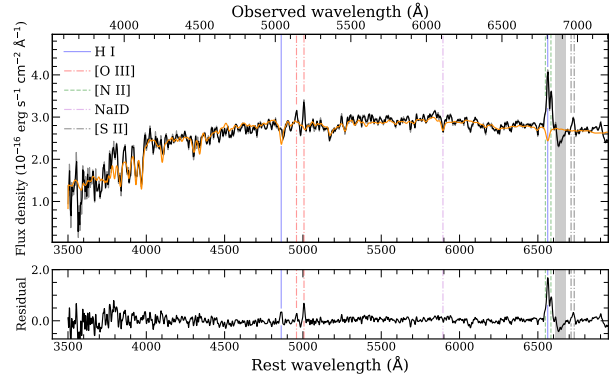


Figure 2 – Optical spectrum of the host galaxy 2MASX J02301709+2836050 obtained with the Nordic Optical Telescope on day 132. *Top*: the black line shows the observed spectrum, while the orange line shows the fit to the stellar continuum provided by STARLIGHT. The vertical lines mark prominent emission and absorption features, which together allow to measure the redshift $z = 0.03657 \pm 0.00002$ ($1 - \sigma$ confidence). *Bottom*: the residuals between the observed data (stellar + nebular spectrum) and the fit (stellar continuum), which single out the nebular emission. The emission line fluxes were measured on the residual spectrum and allow placing the galaxy on the BPT plot (Extended Data Figure. 3).

In the following analysis we assumed $H_0 = 67.36 \text{ km s}^{-1} \text{ Mpc}^{-1}$, $\Omega_\Lambda = 0.6847$, $\Omega_m = 0.3153$ ⁴.

Observations and data analysis

Swift follow-up observations began at 16:07 UTC on June 22 (T0+0.67 d). Due to *Swift*'s Moon observing constraint, subsequent observations were not available until day 4 (June 26). Daily observations of 1 ks exposure were obtained with *Swift* until day 12. A subsequent ToO request was submitted (PI: Guolo) requesting weekly monitoring of this source, which began on day 21 (2022 July 13). The initial observation showed that the source had turned back on in X-rays, but in the following observations on days 27 and 35 it was again below the detection threshold. In order to better quantify the duty cycle, we submitted regular ToO requests (PI: Evans) for daily 1 ks observations, which ran until 2023 March 19 (day 270) when the source entered *Swift*'s Sun observing constraint. Note that we have not *obtained* 1 ks per day; each month proximity to the Moon prevents observations for 3–4 days, and due to the nature of *Swift*'s observing programme, our observations were sometimes shortened or completely superseded by other targets. **Swift-XRT** XRT data were analysed using the on-demand tools of³⁸, via the SWIFTOOLS PYTHON module (v3.0.7). A 0.3–10 keV light curve was constructed, binned to one bin per observation; the soft and hard bands were set to 0.3–0.9 and 0.91–2 keV respectively. Observations 00015231018 and 00015231019 overlapped in time, as did 0001523143 and 0001523144. When this happens the per-observation binning is unreliable, so we built light curves of each of these observations individually, and then replaced the affected bins in the original light curves with those thus obtained. For each run of consecutive upper limit bins, we merged the limits into a single bin, using MERGE-LIGHTCURVEBINS() function in SWIFTOOLS, giving a better measurement of, or limit on, the quiescent flux.

For each observation in which the light curve showed a detection (at the $3-\sigma$ level), we extracted a spectrum, fitting it with a blackbody component absorbed by two absorbers. The first was a TBABS model with N_H fixed at the Galactic value of $1.12 \times 10^{21} \text{ cm}^{-2}$ ³⁹; the second

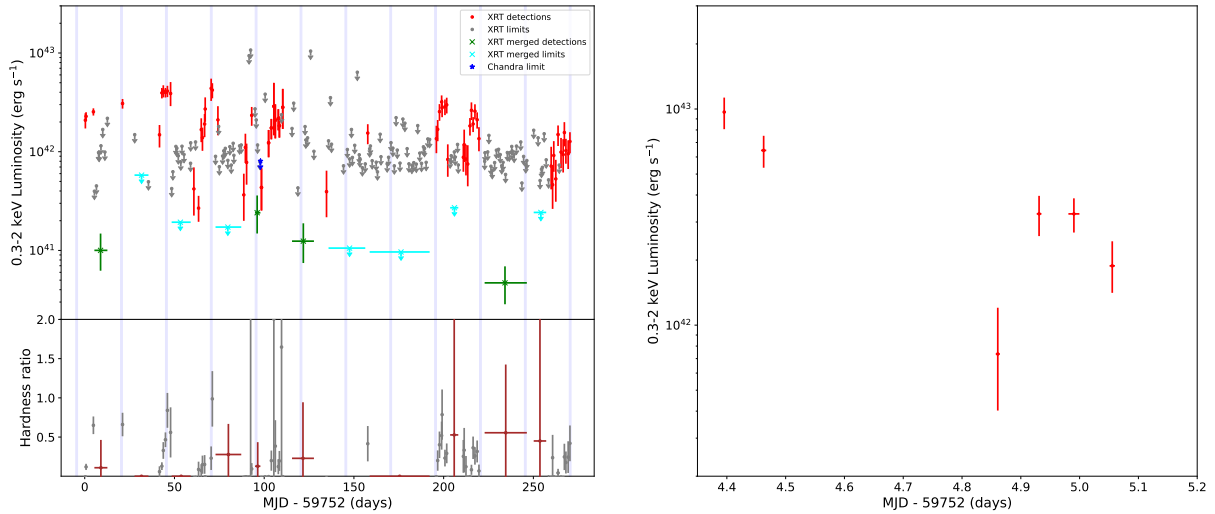


Figure 3 – The temporal evolution of Swift J0230. All error-bars are 1σ significance. **Left:** X-ray time series, binned to one bin per observation. *Top:* 0.3–2 keV luminosity light curve. The red data points marked with dots are the *Swift*-XRT detections; grey arrows are $3\text{-}\sigma$ upper limits from XRT. The dark blue upper limit marked with an asterisk is from *Chandra*. The broad bins marked with crosses were created by combining consecutive XRT non-detections (upper limits in cyan, detections in green); see the Methods section for full details. *Bottom:* The $(0.9\text{--}2)/(0.3\text{--}0.9)$ keV hardness ratio; the spectral hardness is strongly correlated with the luminosity. The vertical bands are at 25-d intervals. **Right:** the light curve of the XRT observation taken on days 4–5, with one bin per spacecraft orbit, showing the rapid decay at the end of the first outburst. All error-bars are at the 1σ level.

was a ZTBABS model with N_{H} free to vary, and the redshift fixed at the value obtained from our NOT spectrum. From these fits we obtained the 0.3–2 keV flux and (given the luminosity distance of 160.7 Mpc) luminosity. The dependence of this luminosity on blackbody temperature, reported in the main paper, is shown in Extended Data Figure. 2. We also obtained for each spectrum the conversion factor from 0.3–10 keV count rate to 0.3–2 keV luminosity, and so converted our count-rate light curve into luminosity. For the detections with too few photons to yield a spectral fit, the upper limits in the light curve and the bins created by merging (above), we used the conversion factor of $7.54 \times 10^{43} \text{ erg ct}^{-1}$ obtained from the discovery observation. The resultant light curve was shown in Figure 3, with the merged bins marked with crosses (and in green/cyan in the online version). To explore the rapid flux decay seen at the end of the first outburst (right-hand panel of Figure 3), we rebinned the data to one bin per snapshot (using the `REBINLIGHTCURVE()` function), converting to luminosity using the same conversion factor (that obtained for the appropriate observation) for each bin.

In order to determine the timescales of the outbursts (Table 1), we defined outbursts as being times where the 0.3–2 keV luminosity was above $3 \times 10^{41} \text{ erg s}^{-1}$ (based on visual inspection of the light curve). We built a new light curve, still with one bin per observation, but in which all bins were created as count-rates with $1\text{-}\sigma$ errors, rather than allowing upper limits (using the `SWIFTOOLS` module with the argument `ALLOWUL=FALSE` passed to the light curve), and then identified each point which was inconsistent with $L = 3 \times 10^{41} \text{ erg s}^{-1}$ at at least the $1\text{-}\sigma$ level. The start and end times of the outbursts were then constrained to being between consecutive datapoints from this sample which were on opposite sides of the $3 \times 10^{41} \text{ erg s}^{-1}$ line. The results are shown in Table 1. We created a Lomb-Scargle periodogram (using the `ASTROPY.TIMESERIES.LOMBSCARGLE` PYTHON package) to search this light curve for periodicity, and find possible peaks centred on 22.1 d and 25.0 d, each with widths of ~ 1 d. To determine their significance we used a bootstrapping method, whereby one ‘shuffles’ the data, randomly redistributing the fluxes (and their errors) among the

time bins, and then recalculates the periodogram. We did this 10,000 times, and then for each trial period in the periodogram identified the 99.7th percentile of power, i.e. the $3\text{-}\sigma$ significance threshold. The result is shown in Extended Data Figure. 1, along with the window function. These two peaks are both clearly above $3\text{-}\sigma$ in significance and not present in the window function.

We also investigated whether with our observing strategy we can rule out short-period variations like those seen in the QPEs reported to date. We simulated a simplistic light curve based on the period of GSN 069 (and including alternating between slightly longer and shorter cycles as in GSN 069). For each snapshot in the real XRT light curve of Swift J0230 we determined the phase of the trial period and set the count rate either to 0.03 ct s^{-1} (‘on’) or 0.001 ct s^{-1} (‘off’); fractional errors were set to typical values from our real light curve. We then constructed the Lomb-Scargle periodogram of this, and repeated the bootstrap approach above. A strong signal was found at the nominal period, confirming that such a signal would have been easily recovered had it been present. Thus we can be confident that there is no short-period modulation like that in GSN 069 present in Swift J0230.

Swift-UVOT UVOT data were analysed using the `UVOTSOURCE` package in `HEASOFT v6.30`. For the pre-outburst data, the location of Swift J0230 was only in the field of view on five occasions. No sign of variability is found in these data, so we summed the images in each filter using `UVOTIMSUM` and extracted mean magnitudes. In the initial discovery observation UVOT gathered data in all filters, but no sign of the outburst is seen, any variability being swamped by the underlying galaxy emission; UVOT magnitudes from this observation and the pre-discovery data are shown in Extended Data Table 1. Due to this lack of variability, subsequent *Swift* observations used the UVOT ‘filter of the day’, which rotates each day between the *u* and UV filters, to preserve the life of the filter wheel. No significant variability is seen. When visually examining the light curve it is tempting to claim some variability in phase with the XRT data, but the magnitude of the variability is much smaller than the errors on the UVOT photometry. To further investigate, we rebinned the XRT light curve to one bin per

snapshot (i.e. the same binning as the UVOT data, which has one exposure per snapshot), and disabled upper limits, forcing a count-rate and $1\text{-}\sigma$ error per bin. For each UVOT filter, we identified the coincident XRT data and then performed a Spearman rank correlation analysis between the XRT and UVOT fluxes. This does not account for the uncertainty on the count-rates, and therefore is likely to overestimate the significance; however, no significant correlation was found at all, with p-values between 0.1 and 0.9, and so more complex correlation mechanisms were not deemed necessary. We also attempted image subtraction, summing all UVOT images in the u filter (that which showed the strongest signs of possible variability) during times of XRT detection and non-detection, before subtracting the latter from the former. No evidence of an excess at the XRT position was seen.

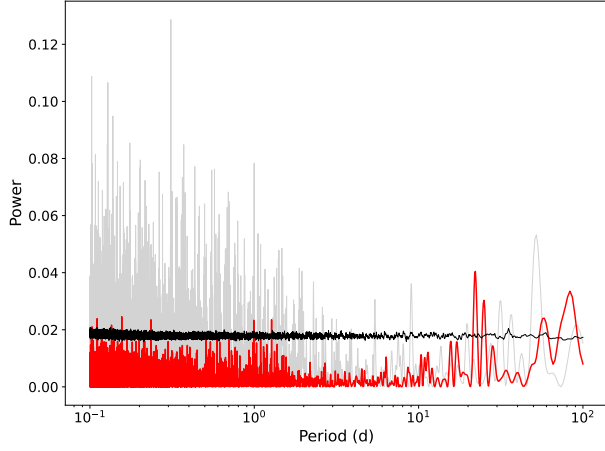
Nordic Optical Telescope Spectroscopy of the host galaxy 2MASX J02301709+2836050 was obtained on 2022 November 1 (day 132). A 2.4-ks optical spectrum was accumulated using the Alhambra Faint Object Spectrograph and Camera (ALFOSC) mounted on the 2.56-m Nordic Optical Telescope (NOT) located at La Palma, Spain. The ALFOSC spectrum was reduced using the spectroscopic data reduction pipeline PyNOT (<https://github.com/jkrogager/PyNOT>). We used a $1.0''$ slit width and Grism #4, covering the wavelength range $\sim 3200\text{--}9600\text{ \AA}$ at resolution $\Delta\lambda/\lambda \approx 360$. The airmass during the observation was of the order of ~ 1.1 . The spectrum is shown in Figure 2, and features prominent $\text{H}\alpha$, $[\text{N II}]$ and $[\text{O III}]$ emission lines, with a common redshift of 0.03657 ± 0.00002 . A weak $\text{H}\beta$ line is also seen. The flux of weaker lines is often affected by the presence of stellar absorption in the continuum. In order to recover the pure nebular fluxes, we fitted the spectrum with the STARLIGHT (<http://www.starlight.ufsc.br/>) software. STARLIGHT fits the stellar continuum, identifying the underlying stellar populations in terms of age and metallicity. Comparing the observed data with the output synthetic spectrum, the pure nebular continuum can be identified, and the emission line fluxes measured accurately.

Based on this analysis, we could build the ‘BPT’ (Baldwin, Phillips & Terlevich) diagram⁴⁰, which is widely adopted to identify the level of nuclear activity in a galaxy. It exploits the ratio of nearby emission lines, minimizing the effects of extinction. The result is shown in Extended Data Figure. 3. 2MASX J02301709+2836050 lies in the locus where low-power AGN, LINERs (Low-Ionization Nuclear Emission-line Region) and star-forming dominated galaxies intersect. A secure classification of 2MASX J02301709+2836050 is therefore not possible, but a powerful AGN is clearly ruled out.

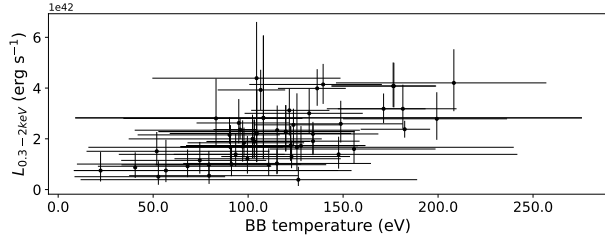
Liverpool Telescope The position of Swift J0230 was observed with the 2 m Liverpool Telescope (LT) optical imager (IO:O) on six different occasions between 2022 Jun 28 and 2022 Aug 26, using the *griz* filters (the first and last epoch were *gri* only). Images were processed using the default IO:O pipeline and downloaded from the LT archive. We co-added exposures and performed basic image subtraction versus Pan-STARRS 1 reference imaging using a custom IDL routine. While a few subtracted image pairs show weak positive or negative residuals at the location of the ~ 18 mag nuclear point source, there is no clear correlation in these residuals between filters or epochs, suggesting minimal contribution of any nuclear transient (or any AGN variability) to the optical flux at the sensitivity level of the LT images. The lack of any residual source at the location of SN 2020rht is unambiguous in all images. Limiting magnitudes of the images (5σ) are given in Extended Data Table 2.

Chandra We requested a 3 ks Director’s Discretionary Time observation of Swift J0230 with *Chandra* (Proposal 23708869). We triggered this on day 93, when the *Swift*-XRT count rate exceeded the approved threshold of 0.02 ct s^{-1} , and the observations were obtained on day 97 (obsID 27470). Our intention was to obtain an accurate (arc-second or better) position of Swift J0230, to be able to say definitively whether

it was associated with the nucleus of its host, the historical supernova, or neither. Unfortunately, this observation occurred during the quiescent/faint part of the 5th outburst, and Swift J0230 was not detected. The $3\text{-}\sigma$ upper limit, converted to $0.3\text{--}2\text{ keV}$ luminosity assuming a 90 eV blackbody with a Galactic absorber, is $L < 8.0 \times 10^{41}\text{ erg s}^{-1}$, consistent with the XRT measurements at the time (Fig. 3).



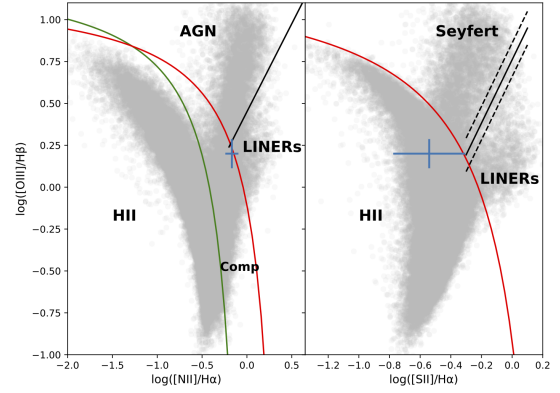
Extended Data Figure 1 – Period analysis of the XRT data of Swift J0230. The Lomb-Scargle periodogram of the per-snapshot binned XRT light curve is shown in red. The window function is in grey and the line marking $3\text{-}\sigma$ significance as a function of period is in black. The two peaks above the $3\text{-}\sigma$ line and not corresponding to window-function peaks are centred on 22.1 d and 25.0 d.



Extended Data Figure 2 – The 0.3–2 keV luminosity and blackbody temperature derived from spectral fits to the XRT observations in which Swift J0230 was detected. A Spearman rank test shows these to be strongly correlated (p-value: 4.5×10^{-6}). The errorbars reflect the 90% confidence intervals on the parameters, obtained using $\Delta C = 2.706$ in the spectral fitting.

Extended Data Table 1 – UVOT photometry from pre-discovery data and the discovery observation.

Filter	Magnitude (AB mag)	Magnitude (AB, discovery obs)
v	15.78 ± 0.07	15.82 ± 0.10
b	16.36 ± 0.07	16.41 ± 0.08
u	17.40 ± 0.07	17.41 ± 0.09
uvw1	18.33 ± 0.08	18.39 ± 0.10
uvm2	18.95 ± 0.08	18.88 ± 0.11
uvw2	18.85 ± 0.07	18.91 ± 0.09



Extended Data Figure 3 – BPT (Baldwin, Phillips & Terlevich) diagram, showing galaxy type (HII star forming region, AGN, LINER, composite) as a function of certain line flux ratios. The line ratios are $[\text{O III}] 5007 / \text{H}\beta$ versus $[\text{N II}] 6583 / \text{H}\alpha$ (left) and $[\text{S II}] 6717,6732 / \text{H}\alpha$ (right). In both panels, the red solid lines are the theoretical models separating star-forming regions and AGN⁴¹. In the left panel, the green line is the demarcation between pure star forming and composite star-forming/AGN regions, as prescribed by⁴². The straight segments separate proper AGN from LINERs (left:⁴³; right:⁴¹). The SDSS galaxy catalogue object density is shown in greyscale⁴⁴ and the position of 2MASX J02301709+2836050 is marked by the blue cross (errorbars are 1σ).

Extended Data Table 2 – Liverpool Telescope upper limits on emission at the position of Swift J0230 after subtracting the galaxy emission (AB magnitudes).

MJD-59752	<i>g</i>	<i>r</i>	<i>i</i>	<i>z</i>
7.20	>20.8	>20.8	>20.9	–
32.20	>21.7	>21.6	>21.7	>21.5
25.15	>20.5	>21.2	>21.4	>21.0
29.18	>20.6	>20.7	>20.6	>20.1
33.21	>22.0	>21.2	>19.6	>17.0
66.12	>21.5	>21.6	>21.5	–

Supplementary Information

Discussion

The nature of the host galaxy, 2MASX J02301709+2836050

A natural question is whether we have detected a new source, or are just seeing normal AGN activity. The first identified QPE occurred in an AGN, the Seyfert-2 GSN 069, but the quasi-periodic nature of the eruptions were not consistent with observed AGN activity¹⁸. Swift J0230 has a much longer (quasi-)period than the previously identified QPEs, but its behaviour remains inconsistent with typical AGN flaring. Rapid variability, such as that seen in the rise and decay of Swift J0230 is sometimes seen in Seyfert galaxies, and recently a narrow-line Seyfert 1 galaxy was shown to undergo a very soft outburst with a similar spectrum to Swift J0230, and a decline similar in timescale to that seen on day 4 of Swift J0230⁴⁵. However, in that object the spectrum hardened as the luminosity declined – the opposite behaviour to that seen in Swift J0230. Further, our optical spectrum (Figure 2), is inconsistent with a narrow-line Seyfert classification: such galaxies show broader spectral lines and strong FeII emission⁴⁶. The BPT diagram (Extended Data Figure. 3) further demonstrates that the optical spectrum is not consistent with a Seyfert, and is only marginally consistent with a weak AGN.

Indeed, there are many objections to classifying 2MASX J02301709+2836050 as a form of AGN. AGN are typically identified by their hard (2–10 keV) X-ray flux, but Swift J0230 was never detected in this band. Summing up all of the 2–10 keV data, 148 ks in total, we obtain a marginal detection (3.2- σ significance, adopting the method of⁴⁷). Assuming a power-law spectrum with a photon index of 1.7, this yields $L_{2-10} = (3.8_{-1.4}^{+1.6}) \times 10^{40}$ erg s⁻¹. This does not alone rule out AGN activity, but does require any AGN to be very weak, consistent with the result of the optical spectrum. Furthermore, the host galaxy does not appear in the ALLWISEAGN catalogue⁴⁸, which contains 84% of all AGN brighter than 2MASX J02301709+2836050. It is present in the WISE catalogue, with colours $W1 - W2 = 0.14$, $W2 - W3 = 3.9$. The $W1 - W2$ colour is much more blue than the AGN shown in the classification plot (fig. 12) of⁴⁹.

The difficulty of explaining the quasi-periodic nature, timescale and luminosity of the outbursts in a weak, non-Seyfert AGN, combined with the above arguments against 2MASX J02301709+2836050 as an AGN, lead us to rule out variability of an existing AGN as a plausible explanation for Swift J0230.

The association with SN2020rht

While the *Swift*-XRT position for Swift J0230 is coincident with the nucleus of the galaxy 2MASX J02301709+2836050, we cannot rule out spatial colocation with SN2020rht. However, as noted in the main article above, it is difficult to identify a mechanism by which SN2020rht could evolve into Swift J0230. Accretion is ruled out on simple energetics grounds: the Eddington luminosity for a stellar-mass black hole is $\sim 10^{38}$ erg s⁻¹, and any theoretical super-Eddington (to the tune of 4 orders of magnitude!) emission would not exhibit the soft, thermal spectrum we observed – and would show strong optical emission along with the X-rays. Magnetar spin-down has been proposed as powering long-lived GRB emission (for example, refs⁵⁰) and can therefore certainly provide sufficient energy; however, existing models are not consistent with Swift J0230, as already detailed above.

We thus regard the near-alignment with SN2020rht as simply a chance occurrence. A detailed calculation of the probability of this is beyond the scope of this paper, especially as the rate of X-ray transients in the Universe is not a well-known quantity; however, a simple consideration is enough to show that such alignments cannot be rare. If the typical supernova rate is 0.01–0.1 per galaxy per year⁵¹, and given

that the XRT localisation accuracy is comparable to or larger than the angular size of a typical galaxy, it follows that the probability of an XRT transient in a given galaxy also lying close to a supernova of up to 2 years old, must be of order a few percent to a few tens of percent.

Comparison of Swift J0230 with similar objects There is a growing collection of systems identified as QPEs, with varying degrees of confidence (and cycles observed)^{18–22}. These systems share various common properties. They have all been discovered in X-rays and show little (if any) variability at longer wavelengths. They are all located in the nucleus of their host galaxies, and have very soft spectra, with almost all emission below 2 keV and capable of being fitted by an absorbed blackbody with temperatures in the ~ 100 –200 eV range. They all exhibit a clear correlation between spectral hardness and luminosity, and have peak luminosities of $L_{0.3-2\text{keV}} \approx 10^{42-43}$ erg s⁻¹. They show outbursts that are approximately, but not strictly periodic. They are typically reported to have black hole masses of $\sim 10^5 M_{\odot}$. These properties are all shared by Swift J0230, with the exception of the timescales. The QPE candidates are all found to have outbursts with durations of minutes to hours, and periods of a few hours; Swift J0230 as noted has a much longer outburst duration and period.

A smaller number of objects have been classified as PNTs^{23–25}. These objects were discovered optically and show much longer periods (> 100 d) but are again repeating events collocated with a galaxy nucleus, this time with black hole masses $\sim 10^8 M_{\odot}$. In the first of these, ASASSN-14ko^{23,24}, no X-ray outburst is seen although the X-ray emission from the host AGN is found to decrease prior to the optical outburst. The second event, AT2018fyk²⁵, does show a strong X-ray and UV outburst which was abruptly terminated, before rising again about 600d later.

A further system, eRASSt J045650.3-203750²⁶, shows similarities to both classes of object. It was discovered via its X-ray outbursts, which are ~ 90 d in duration and occur every ~ 220 d. Spectrally, this object is harder than the QPEs, with notable flux detections above 2 keV. It is again located coincident with a galactic nucleus, with an estimated SMBH mass of $\sim 10^6 M_{\odot}$. In this event, some evidence for UV variability is seen but no optical variation.

All of these objects have been interpreted by the papers cited above as rpTDE events, with differing black-hole masses and donor types. Swift J0230 is clearly most similar to the QPEs and eRASSt J045650.3-203750, but with an outburst duration and period much longer than the former, and shorter than the latter.

The nature of Swift J0230

Here, we discuss the properties of Swift J0230 and estimate physical quantities such as the mass accreted during each outburst. Given the discussion above, we assume that the variability is not caused by activity within a standard AGN disc (by, for example, the mechanisms outlined in^{52,53}). We therefore explore the implications in the context of existing models for accretion of material tidally stripped from stars orbiting near the central black hole^{9,13,15,17}.

If the outbursts are accretion events then the total mass accreted during an outburst is given by:

$$M_{\text{acc}} \sim \frac{E_{\text{ob}} k}{\eta c^2} \quad (1)$$

where E_{ob} is the measured X-ray energy during the outburst, k is a bolometric correction, and η is the radiative efficiency of the accretion process. We can roughly characterise the observed outbursts as lasting ≈ 10 days, with a mean X-ray luminosity of $L_{0.3-2} \sim 3 \times 10^{42}$ erg s⁻¹, thus $E_{\text{ob}} \sim 3 \times 10^{48}$ erg, hence $M_{\text{acc}} \approx 3 \times 10^{27} k / \eta g$. A typical value for the accretion efficiency is $\eta \sim 0.1$ ²⁷. The lack

of observed emission in the UV or optical is consistent with the simple blackbody model fitted to the XRT spectrum, from which we find $k \sim 1$. A correction is needed to account for the absorption, however this change is found (via fitting in XSPEC) to be very small; therefore, $M_{\text{acc}} \approx 10^{-5} M_{\odot}$ is a reasonable estimate of the mass accreted during an outburst.

We can provide an estimate of the black hole mass in Swift J0230 by comparing the measured temperature of ~ 100 eV (1.16×10^6 K) with the peak temperature of a standard accretion disc²⁷. The temperature profile of a standard disc accreting at a rate \dot{M} is

$$T_{\text{eff}}(R) = \left\{ \frac{3GM\dot{M}}{8\pi R^3\sigma} \left[1 - \left(\frac{R_{\text{in}}}{R} \right)^{1/2} \right] \right\}^{1/4}, \quad (2)$$

and thus the maximum temperature reached is

$$T_{\text{max}} = \frac{6^{6/4}}{7^{7/4}} \left(\frac{3GM\dot{M}}{8\pi\zeta^3 R_g^3\sigma} \right)^{1/4} = \frac{6^{6/4}}{7^{7/4}} \left(\frac{3c^6\dot{M}}{8\pi\zeta^3\sigma G^2 M^2} \right)^{1/4} \quad (3)$$

where the innermost stable circular orbit occurs at $R_{\text{isco}} = \zeta R_g$ (with $R_g = GM/c^2$ and ζ ranging from unity for a maximally spinning prograde black hole to 9 for a maximally spinning retrograde black hole), and the numerical pre-factor of $6^{6/4}/7^{7/4} \approx 0.488$ is due to the zero-torque inner boundary condition (see⁵⁴ and references therein for a discussion of discs with non-zero torque boundary conditions).

Taking the total mass accreted during a typical outburst (derived above) of $10^{-5} M_{\odot}$ over a period of 10 d, yields an accretion rate of $\sim 2 \times 10^{22} \text{ g s}^{-1}$. Putting this into Equation 3 gives an estimate for the black hole mass of $M_{\text{est}} \sim 2.4 \times 10^5 (k^{1/2}/\zeta^{3/2}) M_{\odot}$, similar to those reported for QPE sources^{18–20,22}. We note that for the blackbody temperature range of 50–250 eV (Extended Data Figure. 2), the black hole mass estimate ranges from $6 \times 10^4 M_{\odot}$ to $1.5 \times 10^6 M_{\odot}$. With an estimate of the black hole mass, we can now consider the types of system which can produce an rpTDE consistent with the behaviour of Swift J0230.

As discussed in the main paper, the formation of a system in which rpTDE can take place requires the Hills mechanism²⁹, in which a supermassive black hole disrupts a stellar binary system, resulting in one star being ejected and the other being bound to the black hole. In some cases the bound star may have a sufficiently small pericentre distance that it is (fully or partially) disrupted by the black hole, and³⁰ propose this as a route for forming rpTDEs. They show that the orbital period of the bound star is

$$P_{\bullet} \simeq \pi \frac{a_{\star}^{3/2}}{\sqrt{2GM_{\star}}} \left(\frac{M_{\bullet}}{M_{\star}} \right)^{1/2}, \quad (4)$$

where M_{\bullet} is the mass of the black hole, M_{\star} the mass of the primary star. The semi-major axis of the (pre-disruption) binary star system, a_{\star} , is strongly constrained. For $a_{\star} \gtrsim GM_{\star}/\sigma^2 \sim 0.02$ AU (for $M_{\star} = M_{\odot}$ and stellar velocity dispersion $\sigma = 200 \text{ km s}^{-1}$), the binary system would be destroyed by the tidal field of the galaxy centre before reaching the central black hole, while for $a_{\star} \lesssim 0.001$ AU it is hard to fit a main-sequence star of any mass inside the binary orbit. If the progenitor of Swift J0230 were a binary consisting of a compact object (e.g. a white dwarf) and a low-mass main-sequence star, with a semi-major axis of $a_{\star} = 0.005$ – 0.01 AU, and the compact object was ejected during the Hills encounter, then for the low-mass star to enter into a bound orbit around the black hole with the observed ~ 25 d period requires a black hole mass of $M_{\bullet} \sim 4 \times 10^5 M_{\odot}$. This is consistent with the mass estimate derived from the temperature of the X-ray spectrum. It is worth noting that the exact value of the orbital period of the bound star depends somewhat on the details of the Hills capture process. For example, it is possible to get periods of order ~ 25

d with a larger black hole mass (of order $10^7 M_{\odot}$), but as shown in the probability distribution functions (PDFs) displayed in fig. 1 of³⁰ such cases are relatively unlikely with the PDF of the orbital period strongly peaked around the value given by equation 4.

The pericentre distance from the black hole at which the star can be partially disrupted is $\approx 1.6(M_{\bullet}/M_{\star})^{1/3} R_{\star}$ (for example, refs⁵⁵) where R_{\star} is the radius of star. The pericentre distance of the stellar orbit must therefore be $r_p \gtrsim 50R_g$, where $R_g = GM/c^2$ is the gravitational radius of the black hole (assuming a low-mass star and a black hole of mass a few $\times 10^5 M_{\odot}$). This suggests why the outburst period of Swift J0230 is so long compared to the other QPE sources with a similar black hole mass. The QPE sources, with white-dwarf donors, must have pericentre distances that are $\lesssim 5R_g$ to liberate any mass from the white dwarf (indeed in many cases the orbits calculated by¹⁶ have pericentre distances that imply the black hole must be rapidly spinning in the prograde direction to avoid directly capturing the star in a single orbit). Thus, in those sources, any accretion flow that forms will evolve rapidly due to the small circularization radius of the stellar debris, whereas here we have a much larger circularization radius of $\sim 50 - 100R_g$. The viscous timescale for a standard disc with $M_{\bullet} \sim 3 \times 10^5 M_{\odot}$, $\alpha \approx 0.3$ (see ref⁵⁶) and disc angular semi-thickness, $H/R \sim 0.1$, is of the order of hours for radii of order a few R_g , and grows to of the order of days for radii of order $50R_g$. This provides the correct timescales observed for both the QPE sources and Swift J0230. It is therefore possible to explain Swift J0230 as the repeated partial tidal disruption of a solar-type star by a modest-mass black hole, within the framework of a model that can also explain the shorter-period QPEs (white dwarfs orbiting modest-mass black holes) and the longer-period PNTs (main sequence stars around more massive black holes).

Our black-hole mass estimate above was based on the X-ray spectrum as in previous QPE papers (for example, ref¹⁸); however, other methods may also be considered. If we assume that the peak accretion rate is at the Eddington limit then this requires a black hole mass of $1.6 \times 10^5 M_{\odot}$, although this is probably a lower limit as the accretion is more likely to be sub-Eddington. Using the STARLIGHT fits to the optical spectrum (Figure. 2) we can estimate the total stellar mass in the host galaxy 2MASX J02301709+2836050 as $(2.93 \pm 0.94) \times 10^9 M_{\odot}$. The relationship between stellar mass and bulge mass shown by⁵⁷ (see their fig. 8) and⁵⁸ (fig. 4) shows that the expected black hole mass is in the range $\log M_{\text{BH}}/M_{\odot} \approx 5$ – 7 , consistent with the above measurements. Recently,⁵⁹ obtained spectroscopic observations to determine the black hole masses of various QPE hosts using velocity dispersion, finding low masses similar to those predicted by the X-ray temperature approach. This may indicate that QPEs preferentially occur in galaxies with unusually low black hole masses; spectroscopic measurements of 2MASX J02301709+2836050 in order to measure the velocity dispersion will be needed to confirm the black hole mass in this system.

Another interpretation for QPEs that is worth mentioning here is put forward by (see also refs^{8,9}). In this model there are two stars inspiralling towards the black hole due to gravitational wave losses. As the more massive star emits stronger gravitational waves, its orbit shrinks faster such that it can catch up to a lower mass star. This can lead to strong interactions between the stars, stripping gas that can then periodically fuel the accretion flow on to the central black hole. For stars that are orbiting in the same plane but with opposite directions (i.e. one prograde and one retrograde) the stars encounter each other once per orbit, whereas for stars orbiting in the same direction the encounter timescale is many orbits.⁹ predict that the former results in periodicity of order hours and the latter of days. Further⁸ analysed non-coplanar orbits and predicted recurrence times of years to centuries. Thus, this model is capable of explaining the range of timescales from QPEs, to

Swift J0230, to PNTs and beyond. To explain the ~ 25 d variability of Swift J0230 a coplanar set of stars is required. As the stars are likely to encounter the black hole on randomly distributed orientations, a mechanism is required to ensure the stars settle into a coplanar state.⁹ appeal to Type I inward migration through a gaseous AGN disc, which in the case of Swift J0230 may not be present.

Other possible interpretations Other possible explanations for Swift J0230 may be considered, although we find none of them as compelling as the rpTDE model described above. Repeating stellar phenomena such as X-ray binary outbursts can be disregarded on luminosity grounds. Magnetar-powered emission can produce the required luminosity (for example, refs^{6,7,50}). We have above discussed and discarded the possibility of a magnetar connected to the two-year old SN2020rht; more generally, while a magnetar could produce emission with luminosity and spectrum consistent with Swift J0230, the variability observed cannot be explained by this model. The spectral variation observed rules out the possibility of a steadily-emitting magnetar periodically obscured by some absorbing disk or stream, and the absence of strict periodicity rules out binary eclipses.

A class of objects known as ‘Fast X-ray transients’ has been identified in archival data (for example, refs^{60–62}), which undergo relatively rapid X-ray outbursts. However, these are spectrally harder and more luminous than Swift J0230, and have much shorter outbursts (< 50 ks⁶³). Further, they have not been observed to repeat; indeed⁶³ only identify as FXT candidates those objects which were only detected once.

A more promising type of analogous object is HLX-1 in ESO 243-49, which has been proposed as an accreting intermediate mass black hole (IMBH; a black-hole with a mass of $10^{3-4} M_{\odot}$)⁶⁴. This system has a similar peak luminosity to Swift J0230, but a harder spectrum and much longer period. Various models have been proposed to explain this system, including wind accretion⁶⁵ and disc instability⁶⁶, or rpTDE akin to that proposed above¹⁶. As shown above, simple energetics suggests that the amount of matter accreted during a single outburst (and thus stripped from the star every ~ 25 d) is $\sim 10^{-5} M_{\odot}$, orders of magnitude too high to be powered by a stellar wind. In the disc-instability model⁶⁶, the accretion disc is formed by Roche-Lobe overflow, which can provide the requisite amount of mass. In their preferred scenario, the accretion is modulated by a disc wind instability. Furthermore, the HLX outbursts show a fast-rise, slow-decay morphology which is the opposite to that seen for Swift J0230. The differing shape, much shorter period, lack of optical variability, and softer spectra than HLX-1 all pose significant challenges for this interpretation. We therefore conclude that the progenitors of HLX-1 and Swift J0230 are likely to be physically distinct.

We thus conclude that rpTDE is the most likely explanation for Swift J0230, although detailed numerical modelling of the accretion flows is required to confirm whether the deviations from strict periodicity and occasional long quiescent times can be explained by this model.

Declarations

Data Availability All of the *Swift* data are available via the Swift data archives provided in the USA (<https://swift.gsfc.nasa.gov/archive/>), UK (<https://www.swift.ac.uk/archive/>) and Italy (<https://www.ssdsc.asi.it/mmia/index.php?mission=swiftmastr>); they have targetIDs 00014936 and 00015231. Reduced *Swift*-XRT data for this transient are available at <https://www.swift.ac.uk/LSXPS/transients/690>. The *Chandra* data are publicly available via the *Chandra* data archive (<https://cxc.harvard.edu/cda/>), with sequence 704871 and obsID 27470. The NOT data will be available through the NOT public interface after the expiration of the stan-

dard proprietary period; the reduced spectrum is available through the University of Leicester FigShare repository (<https://doi.org/10.25392/leicester.data.c.6444296>). The Liverpool Telescope Data will be available through the Liverpool Telescope public interface after the expiration of the standard proprietary period; the photometry was included in this published article.

Acknowledgments

This work made use of data supplied by the UK Swift Science Data Centre at the University of Leicester. We acknowledge the following funding support: UK Space Agency, grant ST/X001881/1 (PAE, KLP, RAJE-F and AAB). The Science and Technology Facilities Council, grants ST/Y000544/1 (CJN), and ST/W000857/1 (POB). The Leverhulme Trust, grant RPG-2021-380 (CJN). Italian Space Agency, contract ASI/INAF n. I/004/11/5 (SC). European Union’s Horizon 2020 Programme under the AHEAD2020 project, grant 871158 (RAJE-F). European Research Council under the European Union’s Horizon 2020 research and innovation programme, grant 725246 (DBM). The Cosmic Dawn Center (DAWN) is funded by the Danish National Research Foundation under grant No. 140. The Pan-STARRS1 Surveys (PS1) and the PS1 public science archive have been made possible through contributions by the Institute for Astronomy, the University of Hawaii, the Pan-STARRS Project Office, the Max-Planck Society and its participating institutes, the Max Planck Institute for Astronomy, Heidelberg and the Max Planck Institute for Extraterrestrial Physics, Garching, The Johns Hopkins University, Durham University, the University of Edinburgh, the Queen’s University Belfast, the Harvard-Smithsonian Center for Astrophysics, the Las Cumbres Observatory Global Telescope Network Incorporated, the National Central University of Taiwan, the Space Telescope Science Institute, the National Aeronautics and Space Administration under Grant No. NNX08AR22G issued through the Planetary Science Division of the NASA Science Mission Directorate, the National Science Foundation Grant No. AST-1238877, the University of Maryland, Eotvos Lorand University (ELTE), the Los Alamos National Laboratory, and the Gordon and Betty Moore Foundation. LI was supported by grants from VILLUM FONDEN (project number 16599 and 25501) We thank Andy Beardmore for help with the bootstrapping method the period analysis.

Author contributions PAE authored the tools that discovered the event, was PI of the *Swift* and *Chandra* observations, performed most of the X-ray data analysis and led the writing of the article. CJN carried out the theoretical interpretation of the data, and produced the associated text. SC first noticed the automated report of the new transient and classified it as of interest; he was CoI of the *Chandra* observations. PC obtained the NOT spectrum and led the analysis of it, producing Figure 2 and Extended Data Figure. 3. DAP obtained and analysed the Liverpool Telescope data. AAB led the analysis of the UVOT data. KLP carried out some of the XRT data analysis, particularly spectral fitting. SRO supported the UVOT data analysis. RAJE-F was a CoI of the *Chandra* observations and was involved in many discussions concerning the interpretation of the object. DBM arranged for the acquisition of the NOT spectrum and helped with its analysis and interpretation, and was a CoI *Chandra* observations. LI conducted the analysis of the NOT spectrum with STARLIGHT. MRG and PTO offered AGN expertise supporting ruling out AGN activity as the cause of the observed outburst. JPO and BS offered programmatic support and general input. All authors read the text and contributed to its editing.

Competing interests The authors declare no competing interests.

1. Evans, P. A. *et al.* A real-time transient detector and the living Swift-XRT point source catalogue. *Mon. Not. R. Astron. Soc.* **518**, 174–184 (2023). 2208.14478.

2. Evans, P. A., Campana, S. & Page, K. L. Swift J023017.0+283603: A possible tidal disruption event. *The Astronomer's Telegram* **15454**, 1 (2022).
3. Tonry, J. *et al.* ATLAS Transient Discovery Report for 2020-08-13. *Transient Name Server Discovery Report* **2020-2472**, 1 (2020).
4. Planck Collaboration *et al.* Planck 2018 results. VI. Cosmological parameters. *Astron. Astrophys.* **641**, A6 (2020). 1807.06209.
5. Kaaret, P., Feng, H. & Roberts, T. P. Ultraluminous X-Ray Sources. *Annu. Rev. Astron. Astrophys.* **55**, 303–341 (2017). 1703.10728.
6. Metzger, B. D., Vurm, I., Hascoët, R. & Beloborodov, A. M. Ionization break-out from millisecond pulsar wind nebulae: an X-ray probe of the origin of superluminous supernovae. *Mon. Not. R. Astron. Soc.* **437**, 703–720 (2014). 1307.8115.
7. Margalit, B. *et al.* Unveiling the engines of fast radio bursts, superluminous supernovae, and gamma-ray bursts. *Mon. Not. R. Astron. Soc.* **481**, 2407–2426 (2018). 1806.05690.
8. Metzger, B. D. & Stone, N. C. Periodic Accretion-powered Flares from Colliding EMRIs as TDE Imposters. *Astrophys. J.* **844**, 75 (2017). 1705.00643.
9. Metzger, B. D., Stone, N. C. & Gilbaum, S. Interacting Stellar EMRIs as Sources of Quasi-periodic Eruptions in Galactic Nuclei. *Astrophys. J.* **926**, 101 (2022). 2107.13015.
10. Syer, D., Clarke, C. J. & Rees, M. J. Star-disc interactions near a massive black hole. *Mon. Not. R. Astron. Soc.* **250**, 505–512 (1991).
11. Rees, M. J. Tidal disruption of stars by black holes of 10 to the 6th-10 to the 8th solar masses in nearby galaxies. *Nature* **333**, 523–528 (1988).
12. Gezari, S. Tidal Disruption Events. *Annu. Rev. Astron. Astrophys.* **59**, 21–58 (2021). 2104.14580.
13. Zalamea, I., Menou, K. & Beloborodov, A. M. White dwarfs stripped by massive black holes: sources of coincident gravitational and electromagnetic radiation. *Mon. Not. R. Astron. Soc.* **409**, L25–L29 (2010). 1005.3987.
14. Campana, S. *et al.* Multiple tidal disruption flares in the active galaxy IC 3599. *Astron. Astrophys.* **581**, A17 (2015). 1502.07184.
15. King, A. GSN 069 - A tidal disruption near miss. *Mon. Not. R. Astron. Soc.* **493**, L120–L123 (2020). 2002.00970.
16. King, A. Quasi-periodic eruptions from galaxy nuclei. *Mon. Not. R. Astron. Soc.* **515**, 4344–4349 (2022). 2206.04698.
17. Lu, W. & Quataert, E. Quasi-periodic eruptions from mildly eccentric unstable mass transfer in galactic nuclei. *Mon. Not. R. Astron. Soc.* (2023). 2210.08023.
18. Miniutti, G. *et al.* Nine-hour X-ray quasi-periodic eruptions from a low-mass black hole galactic nucleus. *Nature* **573**, 381–384 (2019). 1909.04693.
19. Giustini, M., Miniutti, G. & Saxton, R. D. X-ray quasi-periodic eruptions from the galactic nucleus of RX J1301.9+2747. *Astron. Astrophys.* **636**, L2 (2020). 2002.08967.
20. Song, J. R. *et al.* Possible ~ 0.4 h X-ray quasi-periodicity from an ultrasoft active galactic nucleus. *Astron. Astrophys.* **644**, L9 (2020). 2011.11482.
21. Chakraborty, J. *et al.* Possible X-Ray Quasi-periodic Eruptions in a Tidal Disruption Event Candidate. *Astrophys. J. Lett.* **921**, L40 (2021). 2110.10786.
22. Arcodia, R. *et al.* X-ray quasi-periodic eruptions from two previously quiescent galaxies. *Nature* **592**, 704–707 (2021). 2104.13388.
23. Payne, A. V. *et al.* ASASSN-14ko is a Periodic Nuclear Transient in ESO 253-G003. *Astrophys. J.* **910**, 125 (2021). 2009.03321.
24. Payne, A. V. *et al.* The Rapid X-Ray and UV Evolution of ASASSN-14ko. *Astrophys. J.* **926**, 142 (2022). 2104.06414.
25. Wevers, T. *et al.* Live to Die Another Day: The Rebrightening of AT 2018fyk as a Repeating Partial Tidal Disruption Event. *Astrophys. J. Lett.* **942**, L33 (2023). 2209.07538.
26. Liu, Z. *et al.* Deciphering the extreme X-ray variability of the nuclear transient eRASSt J045650.3–203750. A likely repeating partial tidal disruption event. *Astron. Astrophys.* **669**, A75 (2023). 2208.12452.
27. Shakura, N. I. & Sunyaev, R. A. Black holes in binary systems. Observational appearance. *Astron. Astrophys.* **24**, 337–355 (1973).
28. Fabian, A. C., Pringle, J. E. & Rees, M. J. Tidal capture formation of binary systems and X-ray sources in globular clusters. *Mon. Not. R. Astron. Soc.* **172**, 15 (1975).
29. Hills, J. G. Hyper-velocity and tidal stars from binaries disrupted by a massive Galactic black hole. *Nature* **331**, 687–689 (1988).
30. Cufari, M., Coughlin, E. R. & Nixon, C. J. Using the Hills Mechanism to Generate Repeating Partial Tidal Disruption Events and ASASSN-14ko. *Astrophys. J. Lett.* **929**, L20 (2022). 2203.08162.
31. Nixon, C., King, A., Price, D. & Frank, J. Tearing up the Disk: How Black Holes Accrete. *Astrophys. J. Lett.* **757**, L24 (2012). 1209.1393.
32. Raj, A. & Nixon, C. J. Disk Tearing: Implications for Black Hole Accretion and AGN Variability. *Astrophys. J.* **909**, 82 (2021). 2101.05825.
33. Coughlin, E. R., Armitage, P. J., Nixon, C. & Begelman, M. C. Tidal disruption events from supermassive black hole binaries. *Mon. Not. R. Astron. Soc.* **465**, 3840–3864 (2017). 1608.05711.
34. Predehl, P. *et al.* The eROSITA X-ray telescope on SRG. *Astron. Astrophys.* **647**, A1 (2021). 2010.03477.
35. Yuan, W., Zhang, C., Chen, Y. & Ling, Z. *The Einstein Probe Mission*, 1–30 (Springer Nature Singapore, Singapore, 2022).
36. Chambers, K. C. *et al.* The Pan-STARRS1 Surveys. *arXiv e-prints* arXiv:1612.05560 (2016). 1612.05560.
37. Evans, P. A., Breeveld, A. A. & Oates, S. R. Further Swift observations of the TDE candidate Swift J023017.0+283603. *The Astronomer's Telegram* **15461**, 1 (2022).
38. Evans, P. A. *et al.* Methods and results of an automatic analysis of a complete sample of Swift-XRT observations of GRBs. *Mon. Not. R. Astron. Soc.* **397**, 1177–1201 (2009). 0812.3662.
39. Willingale, R., Starling, R. L. C., Beardmore, A. P., Tanvir, N. R. & O'Brien, P. T. Calibration of X-ray absorption in our Galaxy. *Mon. Not. R. Astron. Soc.* **431**, 394–404 (2013). 1303.0843.
40. Baldwin, J. A., Phillips, M. M. & Terlevich, R. Classification parameters for the emission-line spectra of extragalactic objects. *Publ. Astron. Soc. Pac.* **93**, 5–19 (1981).
41. Kewley, L. J., Dopita, M. A., Sutherland, R. S., Heisler, C. A. & Trevena, J. Theoretical Modeling of Starburst Galaxies. *Astrophys. J.* **556**, 121–140 (2001). astro-ph/0106324.
42. Kauffmann, G. *et al.* Stellar masses and star formation histories for 10^5 galaxies in the Sloan Digital Sky Survey. *Mon. Not. R. Astron. Soc.* **341**, 33–53 (2003). astro-ph/0204055.
43. Schawinski, K. *et al.* Observational evidence for AGN feedback in early-type galaxies. *Mon. Not. R. Astron. Soc.* **382**, 1415–1431 (2007). 0709.3015.
44. Tremonti, C. A. *et al.* The Origin of the Mass-Metallicity Relation: Insights from 53,000 Star-forming Galaxies in the Sloan Digital Sky Survey. *Astrophys. J.* **613**, 898–913 (2004). astro-ph/0405537.
45. Boller, T. *et al.* Extreme ultra-soft X-ray variability in an eROSITA observation of the narrow-line Seyfert 1 galaxy 1H 0707-495. *Astron. Astrophys.* **647**, A6 (2021). 2011.03307.
46. Tarchi, A., Castangia, P., Columbo, A., Panessa, F. & Braatz, J. A. Narrow-line Seyfert 1 galaxies: an amazing class of AGN. *Astron. Astrophys.* **532**, A125 (2011). 1107.5155.
47. Kraft, R. P., Burrows, D. N. & Nousek, J. A. Determination of confidence limits for experiments with low numbers of counts. *Astrophys. J.* **374**, 344–355 (1991).
48. Secrest, N. J. *et al.* Identification of 1.4 Million Active Galactic Nuclei in the Mid-Infrared using WISE Data. *Astrophys. J. Suppl. Ser.* **221**, 12 (2015). 1509.07289.
49. Wright, E. L. *et al.* The Wide-field Infrared Survey Explorer (WISE): Mission Description and Initial On-orbit Performance. *Astron. J.* **140**, 1868–1881 (2010). 1008.0031.
50. Gompertz, B. P., O'Brien, P. T., Wynn, G. A. & Rowlinson, A. Can magnetar spin-down power extended emission in some short GRBs? *Mon. Not. R. Astron. Soc.* **431**, 1745–1751 (2013). 1302.3643.
51. Anderson, J. P. & Soto, M. On the multiplicity of supernovae within host galaxies. *Astron. Astrophys.* **550**, A69 (2013). 1212.4153.
52. Cannizzaro, G. *et al.* Extreme variability in an active galactic nucleus: Gaia16aax. *Mon. Not. R. Astron. Soc.* **493**, 477–495 (2020). 2001.07446.
53. Sniegowska, M., Czerny, B., Bon, E. & Bon, N. Possible mechanism for multiple changing-look phenomena in active galactic nuclei. *Astron. Astrophys.* **641**, A167 (2020). 2007.06441.
54. Nixon, C. J. & Pringle, J. E. Accretion discs with non-zero central torque. *New Astron.* **85**, 101493 (2021). 2008.07565.
55. Coughlin, E. R. & Nixon, C. J. A simple and accurate prescription for the tidal disruption radius of a star and the peak accretion rate in tidal disruption events. *Mon. Not. R. Astron. Soc.* **517**, L26–L30 (2022). 2209.03982.
56. Martin, R. G., Nixon, C. J., Pringle, J. E. & Livio, M. On the physical nature of accretion disc viscosity. *New Astron.* **70**, 7–11 (2019). 1901.01580.
57. Reines, A. E. & Volonteri, M. Relations between Central Black Hole Mass and Total Galaxy Stellar Mass in the Local Universe. *Astrophys. J.* **813**, 82 (2015). 1508.06274.
58. Schutte, Z., Reines, A. E. & Greene, J. E. The Black Hole-Bulge Mass Relation Including Dwarf Galaxies Hosting Active Galactic Nuclei. *Astrophys. J.* **887**, 245 (2019). 1908.00020.
59. Wevers, T., Pasham, D. R., Jalan, P., Rakshit, S. & Arcodia, R. Host galaxy properties of quasi-periodically erupting X-ray sources. *Astron. Astrophys.* **659**, L2 (2022). 2201.11751.

60. Jonker, P. G. *et al.* Discovery of a New Kind of Explosive X-Ray Transient near M86. *Astrophys. J.* **779**, 14 (2013). 1310.7238.
61. Bauer, F. E. *et al.* A new, faint population of X-ray transients. *Mon. Not. R. Astron. Soc.* **467**, 4841–4857 (2017). 1702.04422.
62. Lin, D., Irwin, J. A., Berger, E. & Nguyen, R. Discovery of Three Candidate Magnetar-powered Fast X-Ray Transients from Chandra Archival Data. *Astrophys. J.* **927**, 211 (2022). 2201.06754.
63. Quirola-Vásquez, J. *et al.* Extragalactic fast X-ray transient candidates discovered by Chandra (2000-2014). *Astron. Astrophys.* **663**, A168 (2022). 2201.07773.
64. Farrell, S. A., Webb, N. A., Barret, D., Godet, O. & Rodrigues, J. M. An intermediate-mass black hole of over 500 solar masses in the galaxy ESO243-49. *Nature* **460**, 73–75 (2009). 1001.0567.
65. Miller, M. C., Farrell, S. A. & Maccarone, T. J. A Wind Accretion Model for HLX-1. *Astrophys. J.* **788**, 116 (2014).
66. Soria, R. *et al.* Outbursts of the intermediate-mass black hole HLX-1: a wind-instability scenario. *Mon. Not. R. Astron. Soc.* **469**, 886–905 (2017). 1704.05468.